

The solid curve represents Khalatnikov's final (1952) prediction as given by expression (4), adding to expression (2) the dynamic terms both in viscosity ("second viscosity") and thermal conductivity. Actually this latest work of Khalatnikov's was unknown to the authors until after the experiments had been completed. *The agreement with the experimental results is remarkably good both in magnitude and in temperature dependence.* Khalatnikov did not extend the curve above 2.0°K because above this temperature the density of excitations is so high that the ideal gas approximations for the phonons and rotons can no longer be considered valid. The increase predicted<sup>5</sup> on the basis of the decrease in wave velocity ( $\alpha$  proportional to  $\rho_s/\rho_n v_2^3 \sim 1/v_2$ ) is apparent, however, in the 2.0°K  $\lambda$ -point range.

The data shown within the parallelogram in the upper left-hand portion of Fig. 8 were reported recently by Atkins and Hart<sup>13</sup> for a frequency of 20 kc/sec. Though they plotted values of  $\alpha$  for this frequency on a linear scale, we have for comparative purposes replotted this data on the same  $\log_{10}(\alpha/\omega^2)$  basis originally employed by Khalatnikov. At their lowest temperatures the data clearly indicate the rapid rise in attenuation with decreasing temperature predicted by Khalatnikov. Above 1.4°K, however, the effects of the large beam

spreading at the low frequency employed<sup>16</sup> become more evident. At 1.6°K for example, the geometrical attenuation is apparently already about six times as large as the true attenuation (based on the present results). As a consequence of these large background effects the scatter of their data becomes comparable (see log plot of Fig. 8) to the true liquid attenuation under investigation. By moving Khalatnikov's curve linearly upward to coincide with their points, they demonstrated good agreement within the range covered. Actually they could have obtained absolute determinations from their data below 1.3°K by subtracting the necessary background correction.

#### d. Conclusions

(1) The attenuation of second sound has been measured as a function of temperature and frequency in the submegacycle range. (2) The results are found to agree substantially with the predictions of Khalatnikov. (3) The frequency-squared dependence of second sound attenuation has been established quantitatively. (4) No dependence of second sound attenuation on amplitude has been observed at the low-power levels employed for these measurements.

<sup>16</sup> The geometrical spreading increases as  $1/\nu$  and the second sound attenuation increases as  $\nu^2$ ; thus the ratio of the magnitudes of the two effects ( $\alpha_{\text{true}}/\alpha_{\text{geom}}$ ) varies as  $\nu^3$ . At 100 kc/sec, as opposed to 20 kc/sec, the relative importance of the beam spreading is down by a factor of  $(5)^3=125$ .

## Temperature-and-Field Emission of Electrons from Metals\*

W. W. DOLAN AND W. P. DYKE  
*Physics Department, Linfield College, McMinnville, Oregon*  
 (Received April 9, 1954)

Both the current density and the distribution in energy of electrons emitted from metals are calculated for various combinations of temperature, applied surface electric field, and work function. A wider range of those variables than previously achieved is made possible by use of numerical integration. The integrand is the usual function based on the free-electron theory of metals and the wave-mechanical barrier transmission coefficient of Sommerfeld and Bethe which assumes a classical image force and a plane surface. Results, which are presented in graphical form, are consistent with the Fowler-Nordheim field emission equation for low temperatures, and with the Richardson thermionic emission formula at low fields. Predicted emission at temperatures up to 3000°K is compared with cold emission at fields between  $10^7$  and  $10^8$  v/cm. A qualitative comparison is made between the present results and previous experiments on the transition between field emission and the vacuum arc.

### INTRODUCTION

**E**LECTRONS are emitted from metals under the action of both temperature and electric field. When the temperature is high and the field is low, the process is thermal emission, which is described by the familiar Richardson equation; the effects of intermediate fields on thermal emission are well known as the Schottky

effect. When the field is high and the temperature is low, the process is field emission, described by the Fowler-Nordheim equation; the added effect of intermediate temperature has been considered by several authors, as indicated below.

When both temperature and field are high, the emission process is strongly dependent on both variables and is properly described as neither thermal nor field emission; therefore the descriptive term "temperature-and-field emission," or, in abbreviated form, "*T-F*

\* This work was supported by the U. S. Office of Naval Research.

emission," is used herein. No previous work readily applicable to the general ranges of both variables has been found.

Effects attributed to  $T$ - $F$  emission were seen during the transition from field emission to vacuum arc<sup>1,2</sup> when the electric field was  $7 \times 10^7$  v/cm and the temperature apparently exceeded  $3000^\circ\text{K}$ , which are higher values of the combined variables than those found in earlier works. The experimental methods of reference 2 can be extended to a quantitative study of both  $T$ - $F$  emission and vacuum arc mechanisms, and such study is desirable for several reasons. The properties of  $T$ - $F$  emission are unique, and new or improved electron sources have frequently contributed to advances in both basic science and electronics, the industry in which free electrons are employed. The vacuum arc phenomena have basic importance though they have not been well understood. Furthermore, the arc has important contact with practice; first, it provides a useful means for altering the shape and purity of the microscopic tips of field emitters; second, it sets an upper limit to the field emission current density which can be supplied without damage to the emitter; and third, it is an undesirable form of electrical breakdown in cases where insulation is required.

The present paper concerns a numerical evaluation of the usual integral describing the temperature-and-field dependent emission of electrons from metals. Earlier evaluations of the integral, while in desirable

analytical form, suffered from approximations necessary to that type of solution and from the restriction of the validity of the solution to limited ranges of one or more of the variables. In the present work both the current density and the distribution in energy among the emitted electrons are calculated for electric fields  $F$  encountered in usual field emission experiments, i.e.,  $2 \times 10^7 < F < 7 \times 10^7$  v/cm, and for several temperatures in the range  $0^\circ < T < 3000^\circ\text{K}$ . The effect of several values of work function on current density is considered.

Qualitative comparisons are made between the present calculations and earlier experimental data concerning the transition from field emission to the vacuum arc. The comparison indicates that prior to arc the emitter temperature was at least  $3000^\circ\text{K}$ , a conclusion which strengthens the previously proposed mechanism for arc initiation; measurement of the emitter temperature during intermittent operation has not been otherwise possible because of the microscopic emitter size<sup>3</sup> and transient nature of the heating problem.<sup>4</sup> A more quantitative experimental test of the present calculations will be presented in a forthcoming paper.

From the calculated distribution in energy among emitted electrons, certain conclusions are drawn regarding mechanisms,<sup>5</sup> other than resistive heating,<sup>4</sup> by which the emission process can add energy to, or subtract it from, the metal.

#### THEORETICAL METHOD

The present problem requires knowledge of the values of electron current density and the distribution in energy of electrons emitted from metals at fields up to about  $10^8$  v/cm and temperatures up to and exceeding  $3000^\circ\text{K}$ . Although several early investigators gave attention to this question,<sup>6-8</sup> and the qualitative description of the solution was correctly predicted by Houston,<sup>8</sup> the only careful prior treatment of the general problem was that of Guth and Mullin,<sup>9</sup> which, however, was applicable at the fields in question only for restricted ranges of temperature. A recent contribution by Nakai<sup>10</sup> using numerical methods was of limited usefulness because of its neglect of the image force in defining the surface potential barrier.

Assumptions of the present work include: (1) a simple one-band electron model expressed by the Fermi-Dirac statistics; (2) a smooth metal surface, neglecting effects of atomic scale; (3) a classical image force; (4) the coefficient for transmission of electrons through the

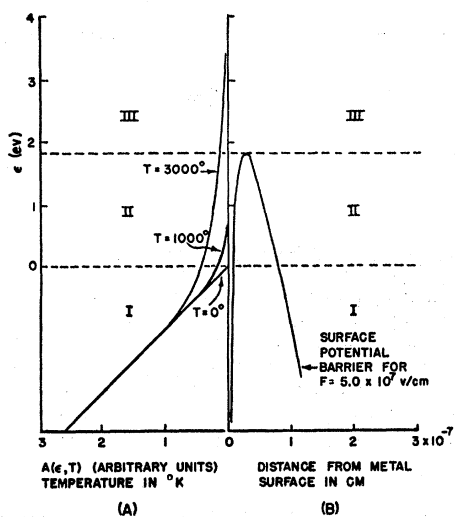


FIG. 1. Schematic drawing showing, on the left, the electron supply function  $A(\epsilon, T)$  for several values of the temperature  $T$  and, on the right, the potential barrier for a typical value of the electric field, the vertical line at 0 representing the metal surface: Region I, below the Fermi level  $\epsilon=0$  (field emission); Region II, between the Fermi level and top of barrier; Region III, above barrier (thermal emission); if emission from Region II is appreciable, the total emission is called  $T$ - $F$  emission.

<sup>1</sup> W. P. Dyke and J. K. Trolan, Phys. Rev. **89**, 799 (1953).

<sup>2</sup> Dyke, Trolan, Martin, and Barbour, Phys. Rev. **91**, 1043 (1953).

<sup>3</sup> Dyke, Trolan, Dolan, and Barnes, J. Appl. Phys. **24**, 570 (1953).

<sup>4</sup> Dolan, Dyke, and Trolan, Phys. Rev. **91**, 1054 (1953).

<sup>5</sup> W. B. Nottingham, Phys. Rev. **59**, 906 (1941).

<sup>6</sup> R. H. Fowler and L. W. Nordheim, Proc. Roy. Soc. (London) **A119**, 173 (1928).

<sup>7</sup> R. A. Millikan and C. C. Lauritsen, Proc. Natl. Acad. Sci. U. S. **14**, 1 (1928).

<sup>8</sup> W. V. Houston, Phys. Rev. **33**, 361 (1929).

<sup>9</sup> E. Guth and C. J. Mullin, Phys. Rev. **61**, 339 (1942).

<sup>10</sup> J. Nakai, Technol. Repts. Osaka Univ. **1**, 213 (1951).

surface potential barrier in the form used by Sommerfeld and Bethe.<sup>11</sup> The latter assumption permits comparison of present results with the generally accepted Fowler-Nordheim equation<sup>12</sup> for cold field emission. Furthermore, as compared with transmission coefficients proposed by other authors,<sup>9,12,13</sup> the coefficient used by Sommerfeld and Bethe has a great advantage in simplicity, while none of the alternate forms found in the literature differed from it by more than a factor of 2 at pertinent energy levels.

Under these assumptions, the current density  $J$  for all fields  $F$  and temperatures  $T$  can be expressed by the single integral

$$J = \int_{-\infty}^{\infty} cA(T, \epsilon)D(F, \epsilon)d\epsilon, \quad (1)$$

where the variable  $\epsilon$  is the difference between the electron energy and the reference energy at the conduction (Fermi) level, and the energies are those associated with the component of velocity normal to the metal surface. The function  $A(T, \epsilon)$  describes the supply of electrons to the surface from the Fermi sea, and  $D(F, \epsilon)$  is the transmission coefficient discussed above. Both are used here in the forms presented in reference 11, namely,

$$\begin{aligned} A(T, \epsilon) &= \ln[1 + \exp(-\epsilon/kT)], \\ D(F, \epsilon) &= \exp[-6.85 \times 10^7 (\phi - \epsilon)^{3/2} f(y)/F]. \end{aligned} \quad (2)$$

Other symbols in Eq. (2) include Boltzmann's constant  $k$ , the work function  $\phi$ , and Nordheim's elliptic function  $f(y)$ <sup>12,14</sup> depending on  $\phi$ ,  $\epsilon$ , and  $F$ . The constant  $c$  in Eq. (1) has the form  $4\pi mkT/h^3$ , where  $h$  is Planck's constant and  $m$  is the mass of the electron.

The function  $A$  is represented graphically in Fig. 1. The vertical line at the center of the figure indicates the metal surface; on the left is the supply function  $A$  for three values of  $T$ , and on the right is the surface potential barrier for a typical field.

Field currents originate from Region I, i.e.,  $\epsilon < 0$ , where the electron supply is large but the barrier transmission coefficient is small, and integration of Eq. (1) over this region (for  $T=0$ ) yields the Fowler-Nordheim equation. Thermionic currents originate from electrons escaping over the barrier (Region III) where the supply is small but the transmission coefficient is large. Integration of Eq. (1) over Region III, for  $F$  small, yields the Richardson equation. For many combinations of  $T$  and  $F$  an appreciable part of the emission originates from energy levels in Region II, i.e., between the Fermi level and the top of the barrier, and is properly neither thermal emission nor field emission. This distinction was pointed out earlier by LePage and DuBridge.<sup>15</sup> In the latter case, the total emission is designated herein

"temperature-and-field emission," which for convenience is abbreviated  $T$ - $F$  emission.

Analytic evaluation of the integral of Eq. (1) over the general range is difficult. In the work of Guth and Mullin<sup>9</sup> it led to the use of certain approximations which limited the range of fields over which the solution was valid at high temperatures. The present work makes use of a simple numerical integration using Simpson's parabolic rule. While this method lacks mathematical elegance as compared with analytic procedures, it is believed that the errors involved are less than those imposed by the approximations of any known analytic method; at the same time the present method offers the advantage of simplicity both in performance and in understanding.

Values of  $A$  and  $D$  were computed for given combinations of  $\phi$ ,  $T$ , and  $F$ . The product  $AD$  was tabulated, and graphed as a function of  $\epsilon$  as exemplified in Fig. 2, which is discussed below. The integration, equivalent to finding the area under such a curve, was extended to a range such that the extreme ordinates of each curve were one percent of the maximum ordinate; thus the contribution from the omitted portion of the curve was negligible. The intervals  $\Delta\epsilon$  used in the process varied, for different temperatures, from 0.1 to 0.3 ev.

## DISCUSSION OF RESULTS

### 1. Energy Distribution of the Emitted Electrons

A few examples of calculated energy distributions for emitted electrons, such as the curves of Fig. 2, have been published by Henderson and Dahlstrom,<sup>16</sup> Mueller,<sup>17</sup> Gomer,<sup>18</sup> and (for the triangular barrier neglecting image force) by Nakai.<sup>10</sup> The first and second of these references were in connection with experimental investigations of the distribution at room temperature; no treatment of the general case was found.

Examination of Fig. 2 reveals the following properties of the distributions: (1) For field emission with  $2 \times 10^7 < F < 7 \times 10^7$  v/cm and low temperature, the maximum of the distribution curve is found near the top Fermi level  $\epsilon=0$ . (2) For  $T$ - $F$  emission at intermediate temperatures beginning near 1000°K, the abscissa of the maximum moves toward higher energies, and the base of the distribution grows broader. The ordinate of the maximum also increases greatly, though this fact is concealed by Fig. 2, in which the amplitudes of all curves are arbitrarily normalized. (3) For  $T$ - $F$  emission at high temperatures, for example 3000°K, the maximum is near the top of the potential barrier.

Another point of view for the interpretation of the combined effect of  $T$  and  $F$  on the energy distribution curves for emitted electrons is offered by Fig. 3. The solid curves show distributions for various fields at a

<sup>11</sup> A. Sommerfeld and H. Bethe, *Handbuch der Physik* (Verlag Julius Springer, Berlin, 1933), Vol. 24, No. 2, p. 441.

<sup>12</sup> L. W. Nordheim, Proc. Roy. Soc. (London) **A121**, 626 (1928).

<sup>13</sup> N. H. Frank and L. A. Young, Phys. Rev. **38**, 80 (1941).

<sup>14</sup> Burgess, Kroemer, and Houston, Phys. Rev. **90**, 515 (1953).

<sup>15</sup> W. R. LePage and L. A. DuBridge, Phys. Rev. **58**, 61 (1940).

<sup>16</sup> J. E. Henderson and R. K. Dahlstrom, Phys. Rev. **55**, 473 (1939).

<sup>17</sup> E. W. Mueller, Z. Physik **120**, 270 (1943).

<sup>18</sup> R. Gomer, J. Chem. Phys. **20**, 1772 (1952).

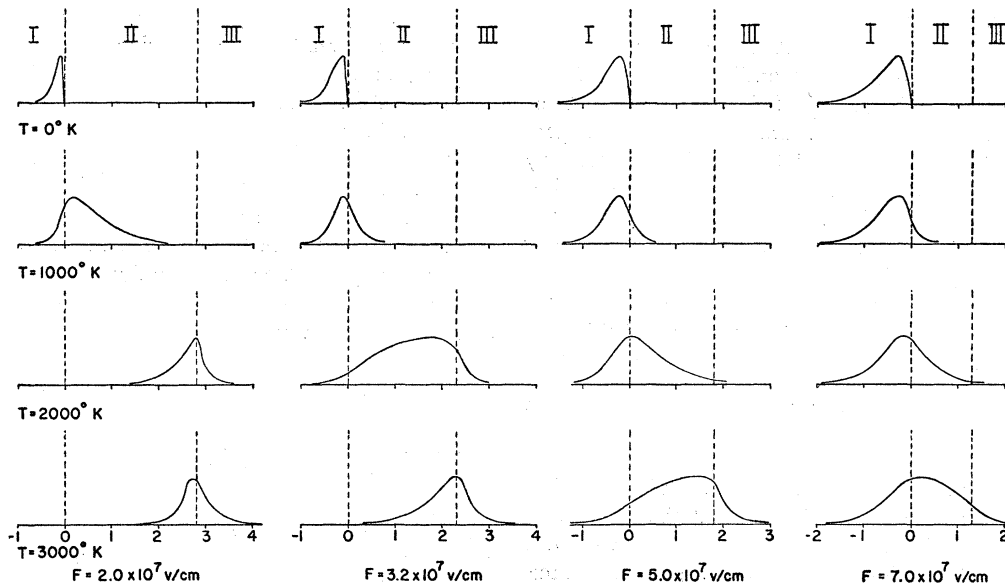


FIG. 2. Theoretical energy distributions for emitted electrons at indicated fields and temperatures, for  $\phi=4.5$  eV, with amplitudes arbitrarily normalized to a common maximum; abscissas  $\epsilon$  in eV relative to the top Fermi level at 0. Regions I, II, and III correspond to those in Fig. 1.

constant temperature of  $3000^\circ\text{K}$ ; these coincide at energy levels above the potential barrier for each field as expected. The dotted curves, on the other hand, indicate distributions for various temperatures at the constant field  $5.0 \times 10^7$  v/cm. In each case, the curves build up to the curve of largest amplitude shown in the figure, that for  $F=5.0 \times 10^7$  v/cm and  $T=3000^\circ\text{K}$ . The

corresponding curve for  $F=10^8$  v/cm and  $T=3000^\circ\text{K}$ , if drawn to the same scale, would have an amplitude more than a hundred times greater than the largest shown in the figure.

## 2. Current Density as a Function of Field and Temperature

Current densities predicted by Eq. (1) for various values of  $F$  and  $T$  at a work function of 4.5 eV (the average value for clean tungsten) are exhibited graphically in Fig. 4. Current density was calculated at five values of  $F$  from  $2 \times 10^7$  to  $10^8$  v/cm for each of the temperatures indicated. It is evident that the enhancement of electron emission due to added thermal energy is much larger at low than at high fields, as was recognized in principle by earlier authors.

It is also clear from Fig. 4 that the temperature effect is slight at values of  $T$  less than  $1000^\circ\text{K}$  for the range of fields shown, but increases rapidly for higher  $T$ . This is of interest in connection with the early experimental attempts to establish such a temperature effect. Millikan and Eyring<sup>19</sup> detected at  $1100^\circ\text{K}$  a slight effect whose magnitude was consistent with the present results; however, de Bruyne<sup>20</sup> failed to observe any effect up to  $1944^\circ\text{K}$ . Earlier work did not benefit from recent techniques which insure clean electrode surfaces and may, therefore, be in doubt in some cases.

The results embodied in Fig. 4 were compared with those computed by the present authors from the formula of Guth and Mullin<sup>9</sup> for the ranges of  $T$  and  $F$  in which the latter is valid. The correspondence between the two

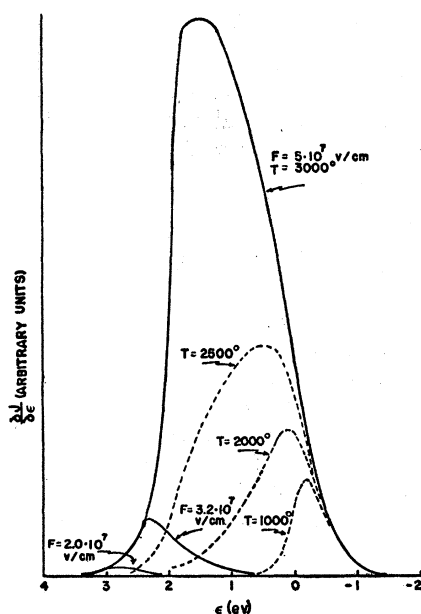


FIG. 3. Energy distributions for emitted electrons with  $\phi=4.5$  eV and at various fields for a constant temperature  $T=3000^\circ\text{K}$  (solid curves); a constant field of  $5 \times 10^7$  v/cm at various temperatures (dashed curves).

<sup>19</sup> R. A. Millikan and C. F. Eyring, Phys. Rev. **27**, 51 (1926).

<sup>20</sup> N. A. de Bruyne, Phil. Mag. **5**, 574 (1928a).

was found to be within the difference introduced by the choices of the coefficient  $D$  in the two cases. Comparison with Nakai's result<sup>10</sup> is not sufficiently informative to merit inclusion here because of the neglect of the image force in his work, and the small number of computations reported. It is worth note that the trend of Nakai's few tabulated values is similar to that given here.

**3. Dependence of Temperature Effect on Work Function**

Calculations heretofore presented assumed a work function  $\phi = 4.5$  ev, the accepted average value for clean tungsten. In order to compare the effect of temperature on current density for several values of  $\phi$  and  $F$ , a limited number of tabulations of  $J$  were made for  $\phi = 6.3$  ev, one of the highest values reported<sup>21</sup> and assigned to the average value for platinum, and  $\phi = 3.0$  ev, a value found experimentally for tungsten partially coated with barium.<sup>22</sup> The trend of these results is exhibited in Fig. 5 in which  $\log_{10}(J/J_0)$  is plotted against  $T$  for the three values of  $\phi$ . The comparison is made at constant field (Fig. 5a) and at constant  $J_0$ , the value when  $T = 0$  (Fig. 5b). In the case of a constant field the effect of high temperature can be interpreted as reducing the disparity between current densities emitted from materials of different work functions; for example, at  $T = 0^\circ\text{K}$  and  $F = 2 \times 10^7$  v/cm, the ratio of current densities for work functions of 3.00 and 6.30 ev is approximately  $10^{16}$ , whereas at  $2000^\circ\text{K}$  it is about  $10^8$  and at  $3000^\circ\text{K}$  less than  $10^6$ .

**CONCLUSIONS**

Several conclusions of a qualitative nature may be drawn from a comparison between the foregoing data and earlier experiments relating to the transition between field emission and the vacuum arc.<sup>1,2</sup> Just prior to arc initiation, an increase in current density over that expected from field emission was observed and attributed to  $T$ - $F$  emission. Comparison of the observed increase with that predicted herein, using the known value of electric field, provides further evidence that the emitter temperature was high just prior to arc. High temperature is thought to be an arc-initiating factor; however, direct measurement of the temperature has not been possible in view of the transient nature of temperature<sup>4</sup> and microscopic size of the heated portion of the cathode tip.<sup>3,4</sup> Quoting from reference 2, "the expected change in [cold cathode] current density was a factor of 1.6 while the observed change in intensity in the [emission pattern] ring was in excess of an order of magnitude based on an estimate aided by a densitometric analysis of the photographic negatives of the emission patterns." An equivalent statement is that

<sup>21</sup> L. A. DuBridge, Phys. Rev. 31, 236 (1928).

<sup>22</sup> Barbour, Martin, Dolan, Trolan, and Dyke, Phys. Rev. 92, 45 (1953).

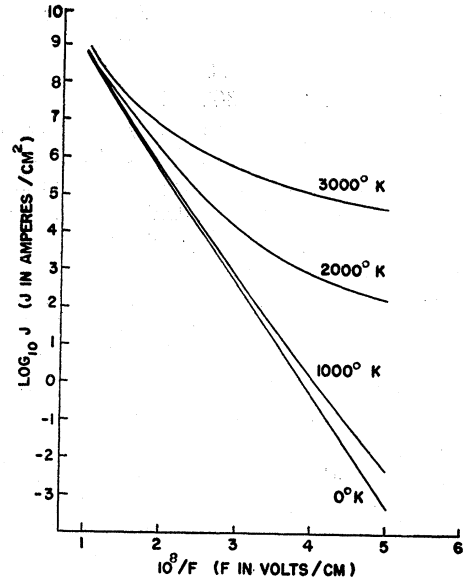


FIG. 4. Graph relating calculated current density  $J$  to electric field  $F$  at various temperatures  $T$ , for  $\phi = 4.5$  ev.

the observed current density was at least a factor of 6 larger than that expected from the cold cathode, the increase being attributed to temperature, which from various data was estimated to exceed  $3000^\circ\text{K}$ . The electric field was known to be  $6.3 \times 10^7$  v/cm at the emitter surface from which the emission pattern ring originated. For these values of  $T$  and  $F$ , Fig. 4 predicts an increase of current density by a factor of 5.0 over the value expected for the cold tungsten cathode, which is in agreement with that observed in the foregoing experiment, within the experimental error. Thus it is

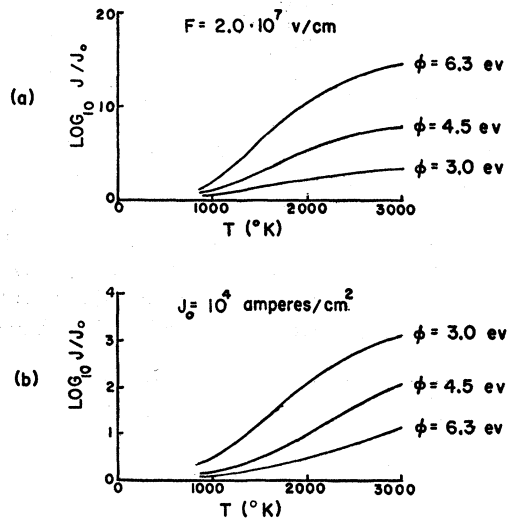


FIG. 5. Graphs showing the dependence of the ratio  $J/J_0$  on temperature  $T$  and work function  $\phi$  at (a) a constant electric field  $F = 2.0 \times 10^7$  v/cm and (b) a constant value for  $J_0 = 10^4$  amp/cm<sup>2</sup>;  $J$  is calculated electron emission current density and  $J_0$  is field current density for  $T = 0^\circ\text{K}$ .

possible to account for the emission pattern ring as due to  $T$ - $F$  emission and to show that the emitter temperature just prior to transition from field emission to vacuum arc was at least 3000°K, a conclusion which strengthens belief in the previously proposed mechanism<sup>1,2</sup> for arc initiation. According to that mechanism evaporated emitter material was proposed as the source of positive ions required to neutralize the known space charge,<sup>22</sup> permitting the large observed current increase which accompanies arc initiation. Resistive heating at the critical current density is adequate to account for the observed temperature increase.<sup>4</sup> A high emitter temperature thus appears fundamental to the transition from field emission to the observed vacuum arc under conditions of excellent vacuum and a clean tungsten cathode surface.

It is interesting to relate the data in Fig. 2 to the thermal behavior of the emitter. The emitter will be cooled during emission from electron energy levels  $\epsilon > 0$  and heated by emission from levels  $\epsilon < 0$ . The former effect is well known in thermal emission and the latter mechanism was proposed by Nottingham<sup>5</sup> for the case of field emission. It is apparent from Fig. 2 that combinations of  $T$  and  $F$  exist such that either process can occur during electron emission from the tungsten cathode. For example, cooling occurs when the mean of the energy distribution curve lies at  $\bar{\epsilon} > 0$ ; in this case, electron vacancies at the mean level  $\bar{\epsilon}$  are replaced by lower energy electrons from the conduction level  $\epsilon = 0$  at the expense of the thermal energy of the emitter. Conversely, as Nottingham has suggested, the metal will be heated when the mean of the energy distribution curve has a value  $\bar{\epsilon} < 0$ . Such energy transfer to or from the cathode, called "emission heating" or "emission cooling" hereinafter, must be added to that supplied by resistive heating.

From Fig. 2 emission heating of the tungsten emitter is appreciable during field emission (low temperature) and may amount to several tenths of an electron volt per electron. Emission heating decreases with increasing temperature ( $T$ - $F$  emission). At low temperatures emission heating usually exceeds resistive heating and will determine an upper limit to the current density which can be drawn if a low cathode-tip temperature is to be maintained. For example, emission heating may preclude the field emission of large current densities from superconducting metals. Gomer and Hulm<sup>23</sup> have re-

ported preliminary studies from superconducting tantalum at low current densities.

For intermediate current densities, for example those obtained with  $F = 5 \times 10^7$  v/cm, emission cooling exceeds resistive heating for all  $T$  above a certain value, thus placing a limit on the value of  $T$  expected from resistive heating for a given current density. This limit can be calculated by the methods of reference 4 when emission cooling is considered along with resistive heating and thermal conduction.

It is interesting to note that emission cooling is small compared with resistive heating during the final stages of the transition between field emission and the vacuum arc, for a typical emitter. Therefore emission cooling appears inadequate to prevent the large emitter temperature increase believed to have initiated the arc for such emitters. Consider, for example, the data from emitter 0-38, reference 2, for which the transition occurred for  $F = 7.4 \times 10^7$  v/cm and  $T = 3000^\circ\text{K}$ , approximately. From Fig. 2,  $\bar{\epsilon}$  may be estimated to have the value 0.2 eV for this case, which represents the energy per electron subtracted from the emitter by emission cooling. On the other hand, resistive heating is about 5 times larger than emission cooling under the same conditions, as may be shown by the methods of reference 4.

A worthy project would be the solution of the transient temperature rise at the field-emitter tip, using the methods of reference 4 with two refinements requiring consideration of (1) resistivity as a function of temperature, (2) emission heating, which is large at low  $T$ , and emission cooling, which is significant under some conditions at high  $T$ . Proper evaluation of the effects of emission heating requires knowledge of its distribution throughout the emitter volume, about which there has been some question.<sup>24</sup>

The data in Fig. 4 can be tested by the experimental techniques used in reference 2 when in addition the emitter is heated from a supply in its support filament. Results of such tests will be reported in a future paper.

The data of Fig. 2 can be tested by the method of Henderson and Dahlstrom<sup>16</sup> together with modifications of their method suggested by Mueller<sup>17</sup> and techniques suggested in the preceding paragraph. Measurement of the distribution in energy among the emitted electrons would provide another method for measuring cathode temperature.

<sup>23</sup> R. Gomer and J. K. Hulm, *J. Chem. Phys.* **20**, 1500 (1952).

<sup>24</sup> G. M. Fleming and J. E. Henderson, *Phys. Rev.* **59**, 907 (1941).